

FINITE DEFORMATION FRACTURE MODELLING USING DIRECT/INVERSE STRONG DISCONTINUITIES

Martin Fagerström^{*†} and Ragnar Larsson^{*}

^{*}Department of Applied Mechanics
Chalmers University of Technology
Hörsalsvägen 7, 412 96 Göteborg, Sweden

[†]E-mail: martin.fagerstrom@chalmers.se

Key words: Partition of unity, Finite deformation, Cohesive zone, Material Crack Driving Force, Dynamic fracture mechanics.

1 INTRODUCTION

In this contribution, we discuss a finite deformation FE-model for crack propagation based on the concept of *partition of unity*, originally introduced by Melenk and Babuška¹, and the developments by Wells *et al.*². The main concept is to consider the total deformation map as a superposition of two fields, one continuous and one discontinuous, leading to a coupled system of equilibrium equations to be solved using a monolithic approach.

To model the fracture behaviour of the material, we distinguish between two different models. Firstly, a cohesive zone model of damage-plasticity type is formulated in the reference configuration, relating the cohesive Mandel traction to a material 'jump', which in turn is related to the direct (spatial) discontinuity^{1†}. Secondly, the Material Crack Driving Force (MCDF) model is formulated as a generalised Griffith criterion based on the material crack driving force, identified as a reaction force at the crack tip in the inverse discontinuity problem⁴, energy conjugated with the virtual crack extension. Both models are compared and discussed with respect to structural response, efficiency, aspects of implementation etc.

Furthermore, we extend the model to account also for dynamical effects, e.g. rapid transient loading which is of great importance in many manufacturing applications and impact loading situations. The intention is to build a theoretical and numerical foundation for further analyses of important dynamic phenomena such as crack arrest, crack branching and rate dependent cohesive behaviour among others. The introduction of inertia effects also rises interesting questions regarding the numerical treatment in terms of efficient and stable time integration algorithms.

^{1†}The formulation in terms of the Mandel traction and the material jump is made to ensure material frame indifference of the model, cf.³

2 KINEMATICS

As a basis for the kinematical description, we consider the direct deformation map which maps points in the material reference configuration, $\mathbf{X} \in B_0$, onto points in the deformed spatial configuration, $\mathbf{x} \in B$ as

$$\varphi[\mathbf{X}, t] = \varphi_c[\mathbf{X}, t] + H_S[S[\mathbf{X}]] \mathbf{d}[\mathbf{X}, t] \text{ with } \mathbf{d} = \mathbf{x} - \mathbf{x}_c \quad (1)$$

where $H_S[S[\mathbf{X}]]$ is the Heaviside function centered at the internal (closed) discontinuity boundary, Γ_S , shown in Figure 1. The argument $S[\mathbf{X}]$ is defined as

$$S[\mathbf{X}] < 0 \quad \mathbf{X} \in D_0^-, \quad S[\mathbf{X}] = 0 \quad \mathbf{X} \in \Gamma_S, \quad S[\mathbf{X}] > 0 \quad \mathbf{X} \in D_0^+ \text{ with } \mathbf{N} = \frac{\partial S[\mathbf{X}]}{\partial \mathbf{X}} \quad \mathbf{X} \in \Gamma_S, \quad \|\mathbf{N}\| = 1 \quad (2)$$

where \mathbf{N} is the normal vector to Γ_S pointing into the region D_0^+ . Note that the discontinuous part, \mathbf{d} , is defined on a subregion D_0 of B_0 (grey area) with assumed Dirichlet boundary conditions along the boundary $\partial D_0^+ \setminus \Gamma_S$.

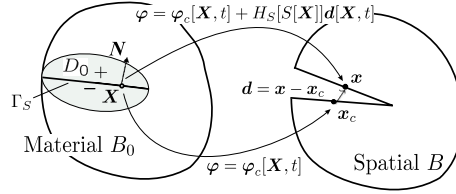


Figure 1: Kinematical representation of the discontinuous direct motion problem.

The pertinent deformation gradient becomes

$$\mathbf{F} = \varphi \otimes \nabla_X = \mathbf{F}_c + H_S \mathbf{F}_d + \delta_S \mathbf{d} \otimes \mathbf{N} \text{ with } \mathbf{F}_c = \varphi_c \otimes \nabla_X \text{ and } \mathbf{F}_d = \mathbf{d} \otimes \nabla_X \quad (3)$$

where $\delta_S[S[\mathbf{X}]]$ is the Dirac delta function.

3 GOVERNING EQUATIONS AND SOLUTION STRATEGY

To arrive at the coupled equilibrium equations, we first consider the strong form of the equation of motion

$$\rho_0 \ddot{\mathbf{u}} - \Sigma_1^t \cdot \nabla_X = \mathbf{b}^{\text{mec}} \quad (4)$$

with Σ_1^t being the first Piola-Kirchhoff stress tensor and \mathbf{b}^{mec} the (applied) mechanics body forces and where the acceleration $\ddot{\mathbf{u}}$ can be subdivided (due to the present kinematical representation) as

$$\ddot{\mathbf{u}} = \ddot{\varphi}_c + H_S \ddot{\mathbf{d}} \quad (5)$$

From Eq. (4), the standard (continuous) form of the principle of virtual work can easily be established, which in turn may be reformulated to the final coupled continuous/discontinuous form by insertion of the discontinuous kinematical representation in

Eqs. (1),(3):

$$(C): \int_{V_0} \Sigma_1^t : \Delta \mathbf{F}_c dV = \int_{\Gamma_0} \Delta \varphi_c \cdot \mathbf{t}_1 d\Gamma + \int_{V_0} \Delta \varphi_c \cdot \mathbf{b}^{\text{mec}} dV - \int_{B_0} \rho_0 \Delta \varphi_c \cdot \ddot{\mathbf{u}} dV \quad (6)$$

$$(D): \int_{D_0} H_S \Sigma_1^t : \Delta \mathbf{F}_d dV + \int_{\Gamma_S} \Delta \mathbf{d} \cdot \mathbf{t}_1 d\Gamma = \int_{D_0} H_S \Delta \mathbf{d} \cdot \mathbf{b}^{\text{mec}} dV - \int_{D_0} H_S \rho_0 \Delta \mathbf{d} \cdot \ddot{\mathbf{u}} dV \quad (7)$$

4 FRACTURE MODELLING

We will present and compare two different models, a cohesive zone model and the Material Crack Driving Force model.

4.1 Cohesive zone model

To model the stress degradation along the internal interface Γ_S , we formulate a cohesive damage-plasticity model based on previous works^{5,4}, thus the nominal traction vector is defined in terms of an effective nominal traction $\hat{\mathbf{t}}_1$ and a damage variable $0 \leq \alpha \leq 1$ as $\mathbf{t}_1 = (1 - \alpha)\hat{\mathbf{t}}_1$. Furthermore, this effective nominal traction is related to the effective Mandel traction $\hat{\mathbf{Q}}$ via $\hat{\mathbf{t}}_1 = \mathbf{F}_c^{-1} \cdot \hat{\mathbf{Q}}$. Finally, $\hat{\mathbf{Q}}$ is expressed in terms of a material jump $\mathbf{J} = \mathbf{F}_c^{-t} \cdot \mathbf{d}$ as $\hat{\mathbf{Q}} = \mathbf{K} \cdot (\mathbf{J} - \mathbf{J}^p) = \mathbf{K} \cdot \mathbf{J}^e$ where \mathbf{K} is a stiffness parameter for the interface and where \mathbf{J}^p and \mathbf{J}^e are the plastic and elastic part of the material jump respectively. The evolution laws for \mathbf{J}^p and α are then defined such that the resulting relation between \mathbf{t}_1 and \mathbf{d} is according to Figure 2.

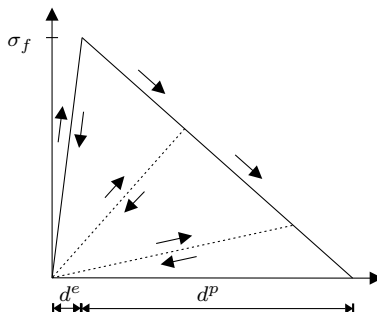


Figure 2: Relation between nominal interface traction and discontinuity.

4.2 Material Crack Driving Force model (MCDF)

The second model proposed is based on the MCDF, \mathbf{P} , identified in the inverse discontinuity problem⁴ as a reaction force at the crack tip, energy conjugated with the virtual crack extension. Interesting properties of this force is that the magnitude corresponds to the value of the J -integral and that the force is aligned in the direction of maximum energy release. Hence, a fracture criterion may be formulated such that the crack is propagated in the direction of the force when the magnitude exceeds a critical value. The drawback of this model is the large mesh sensitivity. However there are techniques to decrease this dependence, e.g. domain integral methods or equivalent.

5 NUMERICAL EXAMPLE

To illustrate the capabilities of the proposed model, we study a simple numerical example in terms of a DCB-test with a pre-defined fracture interface (modelled through the finite elements), shown in Figure 3a, loaded with an increasing loading rate: quasi static (no dynamic effects), $\dot{r} = 6.66$ and 13.33 m/s. The coupled continuous/discontinuous problem is discretised using standard finite element approximations for the two fields and solved with an explicit time integration scheme. Moreover, the continuous material response is considered Neo-Hookean with $E = 3.24$ GPa and $\nu = 0.35$ and the fracture process is governed by the proposed cohesive zone model with mode I fracture energy $G_f^I = 100$ N/m and failure stress $\sigma_f = 20$ MPa. In Figure 3b, the damage distribution along the internal interface at the final load step, corresponding to $r = 0.03$ mm, is presented for the different loading rates. It is noted that a higher loading rates leads to shorter 'fully open' cracks ($\alpha = 1$).

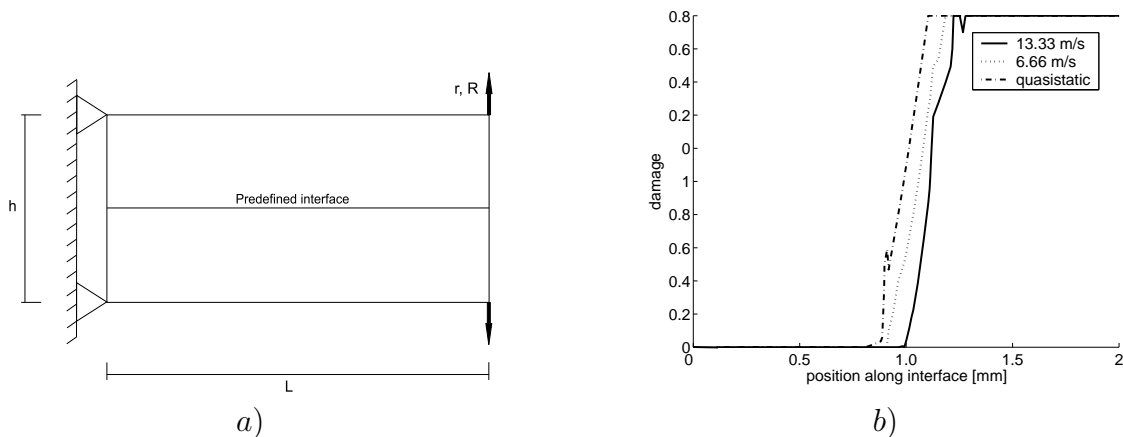


Figure 3: a) Modelled DCB with $h=1$ mm, $L=2$ mm and a thickness of 1mm. b) Damage distribution along Γ_S for different loading rates

REFERENCES

- [1] J.M. Melenk and I. Babuška. The partition of unity finite element method: Basic theory and applications. *Comp. Meth. Appl. Mech. Engng.*, 139:289–314, 1996.
- [2] G.N. Wells, R. de Borst, and L.J. Sluys. A consistent geometrically non-linear approach for delamination. *Int. J. Num. Meth. Engng.*, 54:1333–1355, 2002.
- [3] M. Fagerström and R. Larsson. Theory and numerics for finite deformation fracture modelling using strong discontinuities. *Submitted Int. J. Num. Meth. Engng.*
- [4] R. Larsson and M. Fagerström. A framework for fracture modelling based on the material forces concept with XFEM kinematics. *Int. J. Num. Meth. Engng.*, 62:1763–1788, 2005.
- [5] R. Larsson and N. Jansson. Geometrically non-linear damage interface based on regularized strong discontinuity. *Int. J. Num. Meth. Engng.*, 54:473–497, 2002.